ACA-18-200Rev.Highlighted

Sensor systems for bacterial reactors: A new flavin-phenol composite film for the in situ voltammetric measurement of pH

Charnete Casimero[1], Aaron McConville[1], John-Joe Fearon[1], Clare L. Lawrence[3], Charlotte M. Taylor[2], Robert B. Smith[2] and James Davis[1]*

[1]School of Engineering, Ulster University, Jordanstown, Northern Ireland, BT37 0QB

[2]Chemistry, School of Physical Sciences and Computing, University of Central Lancashire, Preston, PR1 2HE

[3]School of Pharmacy and Biomedical Sciences, Faculty of Clinical and Biomedical Sciences, University of Central Lancashire, Preston, PR1 2HE

Abstract

Monitoring pH within microbial reactors has become an important requirement across a host of applications ranging from the production of functional foods (probiotics) to biofuel cell systems. An inexpensive and scalable composite sensor capable of monitoring the pH within the demanding environments posed by microbial reactors has been developed. A custom designed flavin derivative bearing an electropolymerisable phenol monomer was used to create a redox film sensitive to pH but free from the interferences that can impede conventional pH systems. The film was integrated within a composite carbon-fibre-polymer laminate and was shown to exhibit Nernstian behaviour (55 mV/pH) with minimal drift and robust enough to operate within batch reactors.

Keywords

Riboflavin; Composite; Kefir; Sensor; pH

[1] To whom correspondence should be addressed. T: +44(0)28 903 66407; E: james.davis@ulster.ac.uk

1.0 Introduction

The importance of riboflavin, vitamin B_2, in the maintenance of health is well established and it is known to play a multitude of roles within the body[1–3]. In recent years however, it has begun to garner considerable interest as a key component in the development of electrochemical sensors. Where previously, the focus would have been on its detection[4–10], the spotlight is now being shone on its ability to aid the detection of other molecules associated with disease[11–21]. The prime driver at present relates to the redox chemistry associated with the flavin group which can act as a versatile electrochemical mediator in a range of chemical[21], enzyme[18] and immunosensing[17,19] and microbial[9,12,14,22] systems. These have included the detection of persulfate[20], glutamate[18], human chorionic gonadotropin[17] and hepatitis C[19]. In such cases, the riboflavin is either covalently attached to the base substrate through a chemical linker[16] or has been electropolymerized directly at the electrode[18–21]. The mechanism attributed to the latter is poorly understood [21] and, in most cases, there is considerable degradation in the signal associated with the flavin moiety. Large overpotentials are typically required to induce polymerisation and it is conceivable that the redox groups are compromised during the aggressive oxidative process. We therefore sought to engineer a new flavin analogue which, in contrast to riboflavin, possesses an electropolymerisable phenolic substituent distinct from the core redox centre.

The custom flavin monomer is highlighted in **Scheme 1** and, as with riboflavin, can undergo two core transformations – oxidation and reduction of the flavin (**I** $\rightarrow$ **II** and **II** $\rightarrow$ **I**)[23][21][24]. The inclusion of the phenol substituent however provides a third electrode process through oxidation of the phenol (**I** $\rightarrow$ **III**). It was envisaged that through encouraging polymerisation to proceed in a radical cation process via attack at the pendant phenol ring, rather than directly at the flavin, the characteristic redox transitions (**I** $\rightarrow$**II** $\rightarrow$**I**) could be preserved and then exploited as the basis of an electrochemical sensor. The intention here was to exploit the pH dependence of the redox transitions as a means of indirectly measuring pH. Research into the production of solid state pH sensors has been an increasingly active field in recent years as the need for small, flexible and mechanically robust probes for *in situ* monitoring applications has developed[25–27]. The traditional glass pH probes formats are becoming increasingly incompatible in terms of integration with miniaturised/microfluidic systems or for biomedical

systems where disposability is a prerequisite. The ability to electropolymerize the flavin molecule highlighted in **Scheme 1** is a critical advantage in such contexts as it should enable site specific deposition of the film directly at the electrode irrespective of shape or size. The key challenge however is the retention of the redox signature after film formation has been completed.

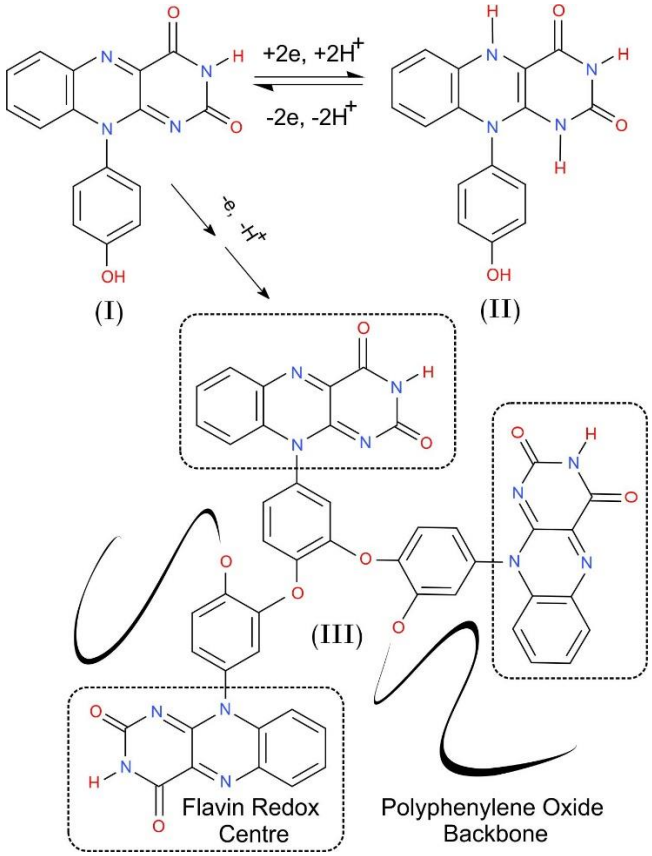

Scheme 1. Redox transition of the flavin unit (III) and the electro-oxidation of the phenolic substituent leading to the production of a polyphenylene oxide polymer (I->III).

The design of the proposed sensor relies on the use of carbon fibre as the electrode – providing a versatile format that can be scaled from single fibre microprobes to large area mats suitable for use in fuel cells. In the present case, the sensor format is based on a pressed carbon fibre mat modified with the flavin polymer and employed as a planar solid state pH sensing element within a microbial reactor designed to produce kefir fermented milk products.

The production and consumption of kefir beverages has a long history spanning hundreds of years with the probiotic nature of the milk ascribed to numerous health benefits which have

been extensively reviewed[28–36]. Cow milk is the traditional feedstock but milk from sheep, buffalo, coconut, rice and soy sources, amongst others, have also been used. Irrespective of source factors (species, geography, feed and season) and processing conditions (pH regulation, temperature, fermentation time) that can influence the nutritional composition of the product and overall flavour[33,36], the underlying taste is usually characterised by a tart/acidic tang. The latter arises from the microbial production of lactic acid during the fermentation process[28]. The degree of acidic aftertaste can affect its palatability and hence monitoring the pH during production can enable greater control over some aspects of the final product characteristic and quality[33,36].

Kefir is produced from the inoculation of the source milk with kefir grains. The latter is a heterogenous mixture of lactic acid bacteria, acetic acid bacteria and yeasts encased in semi hard exo-polysaccharide matrix[30]. The nature of the microbial population will vary greatly depending on production method and, if simply transferred from one batch to another, will inevitably evolve over time. Large scale commercial manufacture typically uses defined starter cultures previously isolated from kefir batches in order to maintain product consistency[29]. Irrespective of the manufacture method, the resulting medium is rapidly transformed to a viscous mixture containing a wealth of small molecules and minerals, proteins, fats, and an ever-expanding kefir grain biomass[28–30,33,35]. This creates a considerable challenge for electrochemical sensors in that, as an interfacial technique, there must be direct contact with the microbial milieu. As the bacterial/yeast communities transform the milk, the pH will inevitably drop – typically from pH 6.5 to pH 3.5. However, the viscosity will rise, as will the possibility of surface fouling. It was anticipated that through anchoring the flavin polymer to the electrode and employing a voltammetric methodology, rather than the simpler and potentially more corruptible potentiometric systems, the influence of the matrix should be minimal.

There is an extensive literature on the development of solid state potentiometric pH sensors with nano materials such as MnO_2[37], IrO_2[38,39], WO_3[40] and ZnO[41] coming to the fore but, in this case, the pH measurement is derived from measuring the peak potential associated with the oxidation of the immobilised flavin group (**Scheme 1, I $\rightarrow$ II**). Voltammetric approaches to the indirect determination of pH have become attractive as they can offer greater selectivity and fast response time in comparison to conventional potentiometric systems[42–45].

A variety of systems employing quinone species[42–44] and nitroso[45] functionalised monomers have been used as the sensing rationale whereby the peak potential is influenced by the prevailing proton concentration. While the shift in the redox potential of riboflavin is well established, this is the first investigation of a flavin being used as an immobilised pH sensor.

2.0 Experimental Details

All chemicals were obtained from Sigma-Aldrich, were the highest grade available and were used without further purification. Electrochemical analysis was carried out using a micro Autolab Type III potentiostat with a standard three-electrode configuration with either a glassy carbon or carbon fibre mat (4 x 4 mm) as the working electrode. Platinum wire served as the counter electrode and a conventional silver/silver chloride (3M KCl, BAS Technicol UK) reference electrode. All measurements were conducted at 22°C ± 2°C. NMR spectra were recorded on a Bruker Fourier 300 (300 MHz) spectrometer. Chemical shifts are reported in ppm relative to solvent residual (^{1}H NMR d_6-DMSO, 2.500 ppm and $CDCl_3$ ppm, 7.26; ^{13}C NMR d_6-DMSO, 39.520 ppm and $CDCl_3$, 77.16). Coupling constants are reported in Hertz (Hz) and are rounded to the nearest 0.5 Hz. Multiplicities are reported as singlets (s), doublets (d) and triplets (t) or a combination of these, peaks that appeared broad due to either H-bonding or restricted rotation are prefixed as broad (br). Low resolution mass spectra were recorded on a Finnigan™ LCQ™ Advantage MAX in ESI mode. Infra-red spectra (1800-800 cm^{-1}) were recorded on a Perkin Elmer Spectrum RX 1 with a Specac Golden Gate™ ATR accessory and values are quoted in wavenumbers.

Kefir Production: Kefir grains were obtained from commercial sources and were incubated in 500 mL (10g live grain kefir at 22°C) batches using cow's milk as the fermentation medium. The carbon fibre probes were placed in the fermentation mixture and pH of the growth medium monitored *in situ* over periods up to 51 hours.

Electrochemical Anodisation: The carbon fibre film was sectioned and mounted in a conventional polyester laminate patterned with a 4 mm square window and thermally sealed[46]. This was done to standardise the electrode area to enable comparison before and after the various modifications. It has become relatively common to electrochemically anodise carbon composite

electrodes in order to counter poor electrochemical behaviour whereby the electro-oxidation (+2 V, 0.1 M NaOH) typically increases exfoliation of the carbon fibre. This has the effect of generating more edge plane sites and introduces various oxygen functional groups (i.e. COOH, OH, C=O)[42].

Flavin Electropolymerisation: Riboflavin was obtained from commercial sources whereas the phenol derivative was custom synthesised. The synthesis of the 10-(4-hydroxyphenyl)benzo[g]pteridine-2,4(3H,10H)-dione was accomplished via modifications to previous methods[47–49]. The reaction summary is highlighted in **Scheme 2** and full details relating to the characterisation of the intermediates can be found in the supplementary information. In summary, p-anisidine (**1**) was reacted with 2-fluoro-1-nitrobenezne (**2**) in the presence of potassium carbonate to yield 4-methoxy-2-nitrodiphenylamine (**3**) which was isolated at the pump in 78% yield. The crude material (**3**) was reduced using zinc dust under acidic conditions, and subsequently treated with alloxan monohydrate (**4**) in the presence of boric acid to yield the 10-(4-methoxyphenyl)benzo[g]pteridine-2,4(3H,10H)-dione intermediate in 93% yield which was demethylated using hydrobromic acid you yield the final derivative (**5**) in 98% yield.

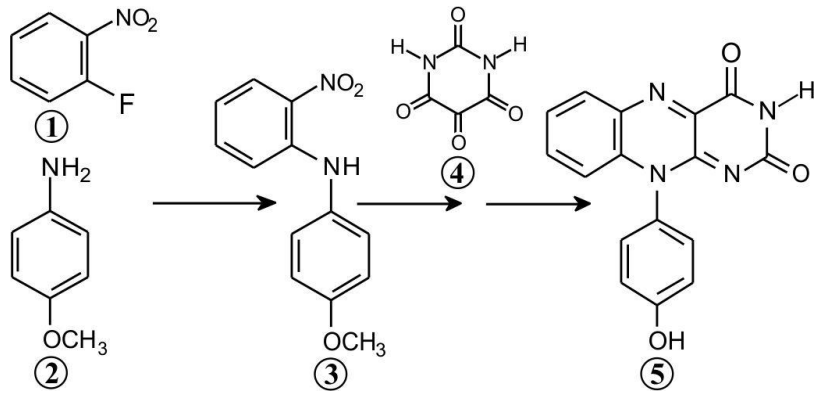

Scheme 2. Preparation of the phenolic flavin derivative

Electropolymerisation was achieved through placing the electrode (glassy carbon or carbon-polyethylene film) into an aqueous solution containing the phenol derivative (150 μM, pH 7). Repetitive scan cyclic voltammetry (+0.2 V -> -0.8 V -> +1 V, 50 mV/s) was used to initiate the electropolymerisation process. Solutions were generally degassed with nitrogen prior to commencing the experiments and run under nitrogen blanket.

3.0 Results and Discussion

The electrochemical properties of the phenolic flavin derivative (I) were compared to riboflavin and the voltammetric responses observed at a conventional glassy carbon electrode are detailed in Figure 1A. In both cases the reduction and oxidation peak processes of the flavin centre (I→II→I) are easily identifiable and exhibit near reversible electrode kinetics. While the phenolic substituent, by nature, will be electron releasing, the effect will be less than the combined influence of the methyl and sugar substituents on the riboflavin and, as such, the reduction of the phenolic flavin derivative occurs at a slightly lower potential. The main difference in the voltammetric profiles however relates to the peak processes observed at +0.81V on the phenolic derivative. The irreversible nature of the peak process and the fact it decreases on consecutive scans (Figures 1B) is consistent with a phenol oxidation process and it is important to note that there is no corresponding electrode process on the riboflavin.

Further examination of the peak processes for the phenolic derivative (Figure 1B) reveals that the flavin peak processes observed at -0.3 V increase in magnitude with increasing scan number. This only occurs when the potential is swept to the positive potentials required to oxidise the hydroxy functionality and thereby induce the formation of oligomeric and polymeric deposits as indicated in Scheme 1 (I→III). When the flavin derivative was cycled with a narrower potential range (+0.2V → -0.8 V) that did not induce the oxidation of the phenol, no increase in the flavin current was observed. Thus, oxidation of the phenol leads to the deposition of the flavin at the electrode with the accumulated material giving rise to sustained increases in the flavin peak magnitude. It is important to recognise at this point that the definition of the flavin peak process remains distinct and stands in contrast to previous reports detailing the electropolymerisation of riboflavin where the peak processes are far from clear[21].

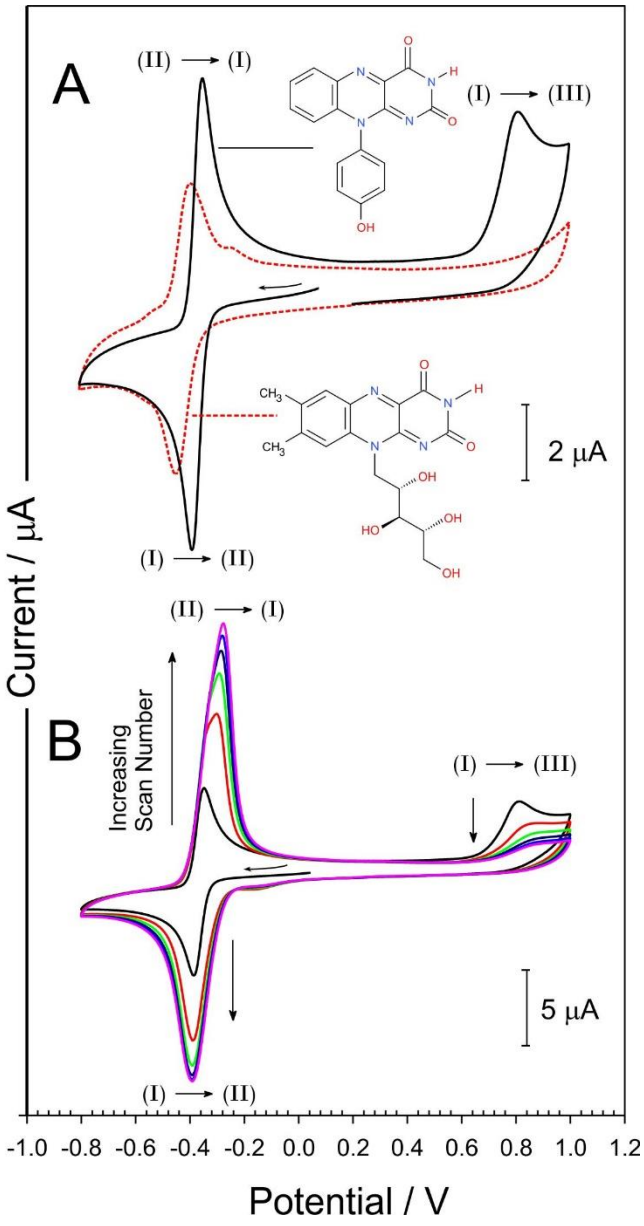

Figure 1. A) Cyclic voltammograms comparing the response of a glassy carbon electrode towards riboflavin and the flavin derivative in pH 7 buffer. B) Five consecutive cyclic voltammograms detailing the electropolymerisation of flavin-phenol derivative in pH 7 buffer. Scan rate: 50mV/s

Further evidence that a polymeric deposit was formed on the electrode surface was obtained through rinsing the electrode and placing in fresh buffer solution. Initial inspection reveals that the flavin peak processes were retained and cyclic voltammograms detailing the response of the immobilised film (in fresh pH 7 buffer) to increasing scan rate are detailed in Figure 2. It can be seen that the peak separation of the flavin unit increases markedly at the higher

scan rates and can be attributed to the slow transfer of counter ions into the film. The variation of peak height with both scan rate and the square root of scan rate are detailed in Figure 2B.

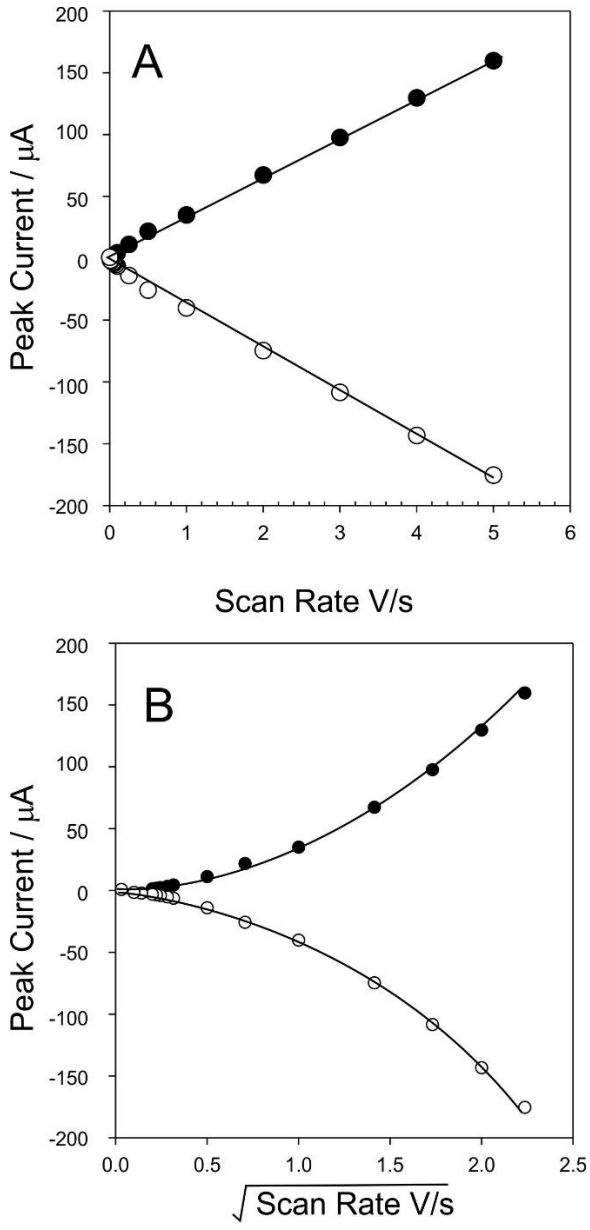

Figure 2. Variation of polyflavin peak heights with scan rate (A) and square root of scan rate (B) recorded on a glassy carbon electrode in pH 7 buffer.

A linear relationship was found with scan rate over the range of 10 mVs^{-1} to 5 Vs^{-1}, indicating a surface-confined electrode process. Roushani and colleagues found similar behaviour

with riboflavin encased as a composite component within graphene quantum dots[20]. Surface coverage (Γ_c) was estimated from the relationship:

$$I_P = \frac{n^2 F^2 A \Gamma_C}{4RT} v$$

where I_p is the peak height, v is the sweep rate, A is the effective surface area (0.071 cm^2) of the glassy carbon electrode and the other symbols have their usual meaning. From the slope of cathodic peak currents vs. scan rate, the calculated surface concentration of the poly flavin compound was found to be 1.32×10^{-10} mol cm^{-2}.

Given the apparent stability of the redox processes shown in Figure 2 after insertion in fresh buffer, the next step was to determine if the flavin film could be transferred to an electrochemically treated carbon fibre mesh electrode. The flavin monomer was electropolymerized using the same approach employed with the glassy carbon electrode and the voltammetric profiles obtained were analogous to the scans highlighted in Figure 1B. The flavin modified carbon fibre electrode was removed and the influence of pH on the peak responses assessed. In this instance, square wave voltammetry was used to enable a more accurate determination of the peak potential and to minimise the effect of oxygen. The scans were initiated at -0.8 V which, as indicated in Figure 1, is sufficiently negative to induce the reduction of the flavin centre. The scan is then swept towards more positive potentials whereby the flavin is re-oxidised. The voltammetric responses obtained in buffers of varying pH are detailed in Figure 3. In each case, a well-defined oxidation peak is obtained and moves towards more negative potentials with increasing pH. The relationship between peak position and pH was found to be near Nernstian with a typical slope of 55 mV/ pH unit (E / V = 0.055 pH + 0.077; N = 7; R^2 = 0.999). This is similar to previous reports on the use of riboflavin-graphene quantum dots[20].

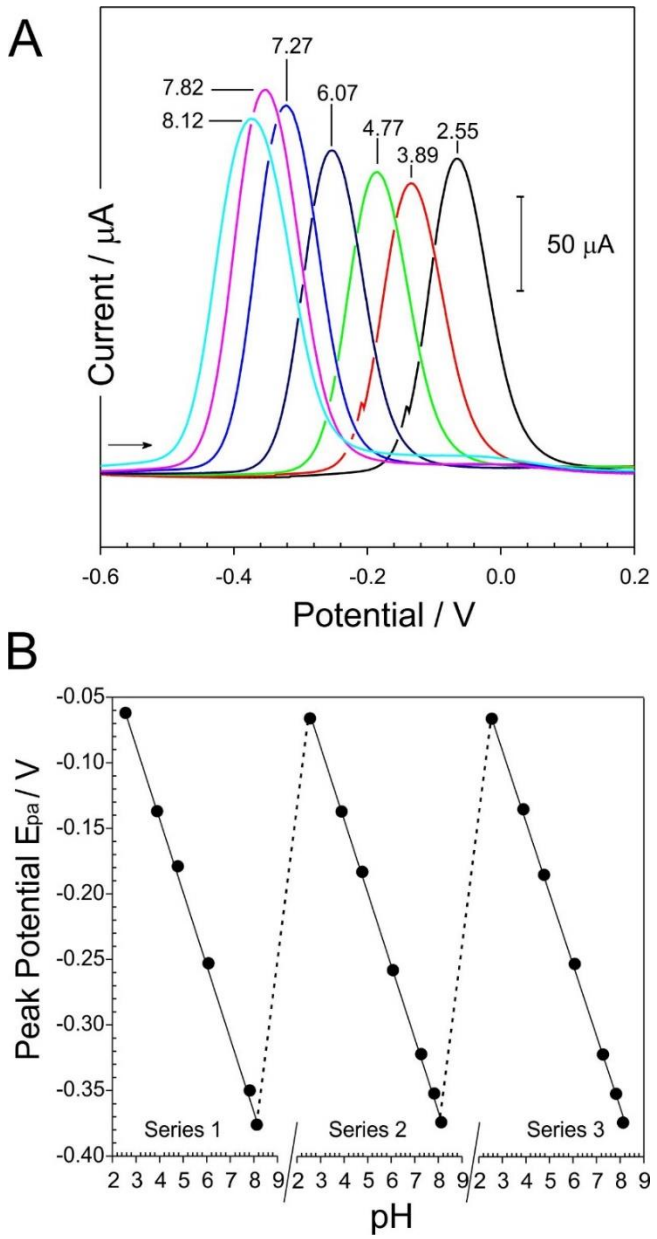

Figure 3. A) Square wave voltammograms detailing the response of the flavin modified carbon fibre mesh in buffers of varying pH. B) Influence of pH on oxidation peak potential over three cycles (Each pH analysed in triplicate - total 63 scans).

The robustness of the modified film towards periodic scanning - a prerequisite when monitoring the pH change within a batch process taking at least 24 hours to complete – was assessed through cycling the electrode through a series of three pH sequences – each sequence ranging from pH 2.55 to pH 8.12. Square wave voltammograms were recorded in triplicate for

each pH buffer and the entire process repeated a further two times to establish the reversibility of the pH changes on going from low pH to high pH and back again (Figure 3B). It was anticipated that this process would also identify any potential drift should the integrity of the redox centres within the film be compromised as a consequence of the repetitive cycling. The latter can be common in quinoid systems where the oxidised centre can be prone to attack from hydroxyl ion in moderately alkaline conditions. Given the data highlighted in Figure 3B, it is clear that the pH sensing capabilities are reversible with a drift of only 4 mV. The height of the peak was however found to be affected with a reduction in the magnitude in the range of 20% over the course of 63 scans.

It must be acknowledged that operation within a clean buffer solution presents little chemical or physical challenge to the system, therefore the next phase was to examine the performance of the carbon fibre – flavin composite in the kefir matrix – from the initial inoculum to the final production of the kefir milk. During this time, it was anticipated that there would be a significant increase in the biomass within the batch which could foul the electrode. The latter was confirmed through examining the electrode fibre network before immersion and after 51 hours fermentation. The electron micrographs obtained are shown in Figure 4 and highlight how the microbial biomass permeates through the fibre network.

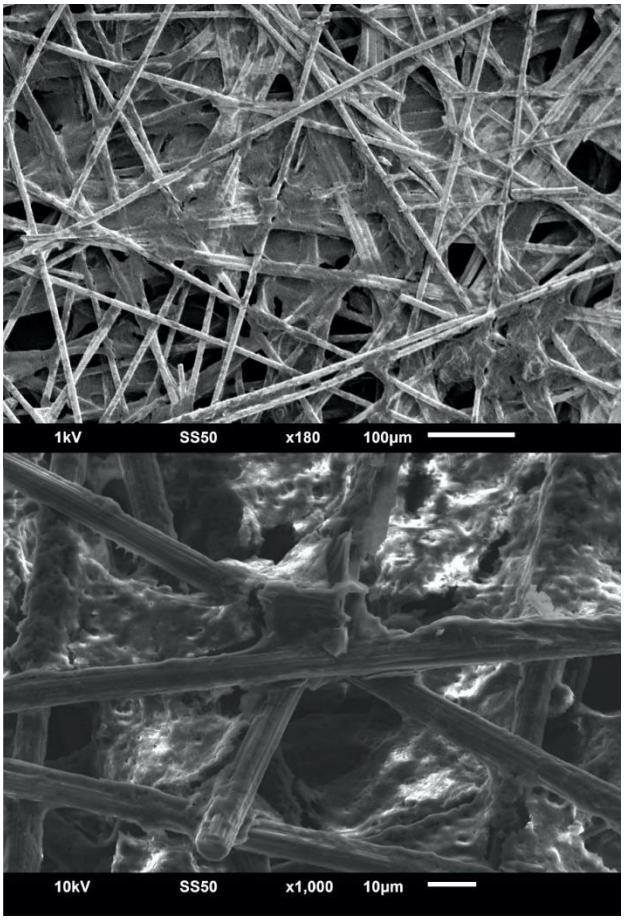

Figure 4. Scanning electron micrographs of the carbon fibre network after incubation in Kefir mixture.

Square wave voltammograms detailing the response of anodised carbon fibre electrodes with and without the flavin polymer film in the kefir mixture before and after production are compared in Figure 5. Examining the response of carbon fibre electrodes without the flavin layer reveals the presence of a small but distinct oxidation peak – initially at -0.413 V which then moves to -0.231 V at the end of production (51 hrs). This is ascribed to the presence of riboflavin which is endogenous to the milk mixture. The pH of the batch switches from pH 6.18 to pH 3.68 when complete.

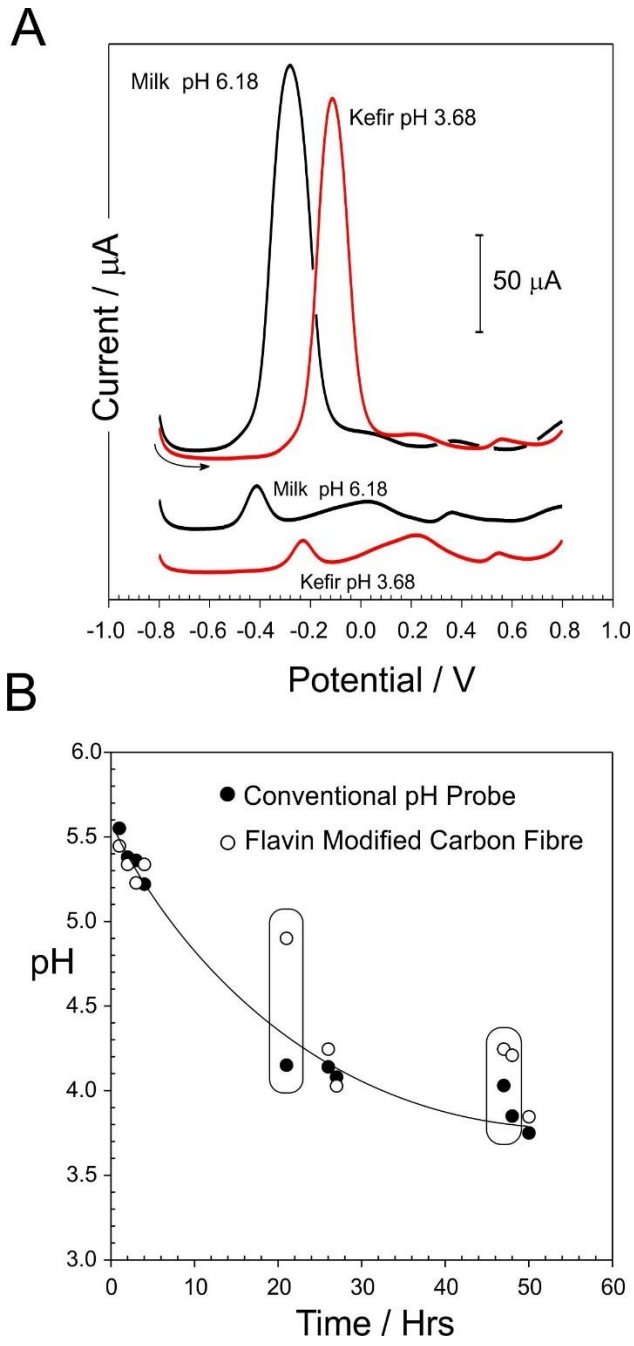

Figure 5. A) Square wave voltammogram detailing the response of a poly flavin modified carbon-fibre electrode in kefir at the start and end of the fermentation cycle. B) Comparison between the conventional glass pH probe and the flavin modified electrode within the kefir mixture over a period of 50 hours. Each point is the average of 3 scans.

It can be seen from the data presented in Figure 5 that while the pH recorded at the flavin modified fibre follows that obtained with the conventional glass probe, there are anomalies. The

latter are highlighted in Figure 5 and it is noteworthy that on both occasions, significant deviations occur only after a period in which the electrode has been dormant for over 12 hours. In contrast, repetitive scanning, in which the delay between each scan is short, results in close agreement with the standard pH probe. It should also be noted that upon recommencing the measurements – the response of flavin modified probe soon recovers to match the standard probe. It is likely that during the dormant phases – microbial colonisation of the probe (as indicated in Figure 4) initially compromises the response with the pH recorded reflecting the local environment arising within the biofilm at the film interface. Further modification of the probe with a permselective barrier to minimise fouling could be considered but film formation on the barrier may still lead to a discrepancy between the internal void and the bulk. Scanning with increased frequency however appears to negate such an approach (at least in this instance) an is shown to minimise the deviations from the control pH. This could be attributed to the redox transitions at the surface and the corresponding physical swelling through the flux of counter ions. Nevertheless, biofilm formation is apparent after the 51 hours and, while this is arguably beyond the typical fermentation timespan used in Kefir consumer products, it could be problematic when considering translation to other microbial systems (i.e. fuel cells)[50].

In principle, it is possible to utilise the bare, anodised carbon fibre as a means of measuring the riboflavin directly within the kefir milk sample and exploit the fact that the oxidation peak process moves with pH. The shift in the riboflavin peak potentials with pH is well established[20]. There are, however, several issues with this approach. It assumes that riboflavin will always be present in the milk feedstock and at a level which can be easily detected. Switching to other milk sources such as soy or coconut or sugar feeds where there may be less or no riboflavin would clearly nullify this approach[28,35]. Examination of the voltammogram in Figure 5 also highlights the fact that although the riboflavin peak is distinct in both the initial and final mixtures, the magnitude of the peak is similar to the other, unascribed, components within the mixture (the broad peak at +0.25V). It is possible that even with minor changes in the composition of the milk feed (i.e. the introduction of flavours or other additives, that the endogenous riboflavin peak could be obscured. The magnitude of the immobilised flavin stands in marked contrast to the solution riboflavin and overcomes any issue with changes in the nature and composition of the starter mixture.

The development of new pH sensing methodologies and electrode modifiers than can confer pH selectivity is an ever-present challenge and continues to capture the attention of

researchers. A summary of the more recent advances in the field are detailed in Table 1 along with a comparison of this work. It is notable that, while there is a wide variation in the nature of the electrode modifier/technology, validation of the systems within real matrices is often problematic. The flavin system investigated here demonstrates a near Nernstian response and, while the key parameters are comparable to many of those highlighted in Table 1, it is important to note that it has been tested within a complex and changing medium.

Table 1. Comparison of electrode modifiers / pH detection methodologies

Modifier	Type[a]	Sensitivity mV/pH	pH Range	Test Medium	Ref.
$CeTi_xO_y$	P	89.8	2-12	N/A	[51]
RuO_2/Nafion	P	55.2	2-6	Beverages	[52]
IrO_x / Pt	P	64	1-13	Corrosion	[53]
ERGO Polyaniline / Nafion	P	55	2-9	Fermentation	[54]
CuO nanorods	C	0.64 μF/pH	5-8.5	N/A	[55]
Graphite/polyurethane	P	11.13	5-9	Sweat	[56]
WO_4/WO_3	P	56	2-10	N/A	[57]
Graphene - Polyaniline	A	139 μA/pH	1-5, 7-11	N/A	[58]
NiO	P	63	1-13	N/A	[59]
ZnO/W	P	46	2-9	CSF	[60]
$Ni_3(PO_4)_2{\cdot}8H_2O$	P	34.8	4-7	Sweat	[61]
Carbon-quinone	V	73	2-8	Saliva	[62]
Pt-IrO_x	P	56	4-9	Biofilm	[63]
Si EGFET	P	56	2-12	N/A	[64]
ZnO	P	43	2-9	Tumor Cells	[65]
Polyaniline	V	50	4-10	Wound fluid	[66]
Poly Dopamine	V	58	1-12	N/A	[67]
Poly Flavin	V	55	2-8	Fermentation Reactor	This Work

[a] where C = capacitance; P = potentiometric; V = voltammetric; A = amperometric;
EGFET = extended gate field effect transistor; ERGO = electrochemically reduced graphene oxide.

4.0 Conclusions

A solid state pH sensor based on an engineered flavin redox polymer has been shown to be capable of operating within a microbial reactor. Critically, the system provides a clear, unambiguous signal within a chemically complex medium with the redox peaks residing within a potential region where there are few competing processes. The application of square wave voltammetry enables the accurate determination of peak position from which the pH can be

readily computed. The system is reagentless and exhibits reversible characteristics over the pH range 2-8 with minimal drift. A key feature is the ability to identify and measure the analytical peaks within the need for solution degassing. The flavin polymer was immobilised on an inexpensive carbon fibre network and while deployment and, indeed replacement, is more economically acceptable, it could be envisaged that the system could be translated to screen printed systems to facilitate the development of disposable sensor systems.

Acknowledgements

The authors are pleased to acknowledge financial support from the Department of Employment and Learning (DEL) Northern Ireland and the University of Central Lancashire Innovation and Enterprise for supporting this work.

Electronic Supporting Information

Detailed descriptions of the synthesis of the phenolic flavin compound and the associated chemical characterisation data for each of the intermediates are available.

Declaration of Interests

Conflicts of interest: none

Author Contributions:

Electrochemical analysis of flavin: Charnete Casimero, John-Joe Fearon

Physical characterisation/modification of carbon fibre: Aaron McConville

Synthesis of intermediates: Charlotte M. Taylor

Supervision and characterisation of synthesis/products: Robert B. Smith, Clare L. Lawrence

Supervision of overall project and compilation of manuscript: James Davis

References

[1] K. Porter, C.F. Hughes, L. Hoey, M. Ward, K. Moore, J.J. Strain, A. Molloy, C. Cunningham, M. Casey, K. Pentieva, H. McNulty, Investigation of the role of riboflavin, vitamin B6 and MTHFR genotype as determinants of cognitive health in ageing, Proc. Nutr. Soc. 75 (2016) E114. doi:10.1017/S0029665116001294.

[2] K. Thakur, S.K. Tomar, A.K. Singh, S. Mandal, S. Arora, Riboflavin and health: A review of recent human research, Crit. Rev. Food Sci. Nutr. 57 (2017) 3650–3660. doi:10.1080/10408398.2016.1145104.

[3] H.J. Powers, Riboflavin (vitamin B-2) and health 1 , 2, (2003) 1352–1360.

[4] D. Riman, A. Avgeropoulos, J. Hrbac, M.I. Prodromidis, Sparked-bismuth oxide screen-printed electrodes for the determination of riboflavin in the sub-nanomolar range in non-deoxygenated solutions, Electrochim. Acta. 165 (2015) 410–415. doi:10.1016/j.electacta.2015.03.056.

[5] L.C. Gribat, J.T. Babauta, H. Beyenal, N.A. Wall, New rotating disk hematite film electrode for riboflavin detection, J. Electroanal. Chem. 798 (2017) 42–50. doi:10.1016/j.jelechem.2017.05.008.

[6] F. Karimian, G.H. Rounaghi, M. Mohadeszadeh, Electrochemical determination of riboflavin using a synthesized ethyl[(methythio)carbonothioyl] glycinate monolayer modified gold electrode, J. Anal. Chem. 71 (2016) 1057–1062. doi:10.1134/S1061934816080062.

[7] R. Gupta, P.K. Rastogi, U. Srivastava, V. Ganesan, P.K. Sonkar, D.K. Yadav, Methylene blue incorporated mesoporous silica microsphere based sensing scaffold for the selective voltammetric determination of riboflavin, RSC Adv. 6 (2016) 65779–65788. doi:10.1039/C6RA12336H.

[8] A. Kowalczyk, M. Sadowska, B. Krasnodebska-Ostrega, A.M. Nowicka, Selective and sensitive electrochemical device for direct VB2 determination in real products, Talanta. 163 (2017) 72–77. doi:10.1016/j.talanta.2016.10.087.

[9] Y.Y. Yu, J.X. Wang, R.W. Si, Y. Yang, C.L. Zhang, Y.C. Yong, Sensitive amperometric detection of riboflavin with a whole-cell electrochemical sensor, Anal. Chim. Acta. 985 (2017) 148–154. doi:10.1016/j.aca.2017.06.053.

[10] H. Zhang, Y. Gao, H. Xiong, Sensitive and Selective Determination of Riboflavin in Milk and Soymilk Powder by Multi-walled Carbon Nanotubes and Ionic Liquid [BMPi]PF6 Modified Electrode, Food Anal. Methods. 10 (2017) 399–406. doi:10.1007/s12161-016-0598-z.

[11] M. Roushani, F. Shahdost-Fard, A novel ultrasensitive aptasensor based on silver nanoparticles measured via enhanced voltammetric response of electrochemical reduction of riboflavin as redox probe for cocaine detection, Sensors Actuators, B Chem. 207 (2015) 764–771. doi:10.1016/j.snb.2014.10.131.

[12] H. Bao, Z. Zheng, B. Yang, D. Liu, F. Li, X. Zhang, Z. Li, L. Lei, In situ monitoring of Shewanella oneidensis MR-1 biofilm growth on gold electrodes by using a Pt microelectrode, Bioelectrochemistry. 109 (2016) 95–100. doi:10.1016/j.bioelechem.2016.01.008.

[13] C. Sumathi, P. Muthukumaran, P. Thivya, J. Wilson, G. Ravi, DNA mediated electrocatalytic enhancement of [small alpha]-Fe2O3-PEDOT-C-MoS2 hybrid nanostructures for riboflavin detection on screen printed electrode, RSC Adv. 6 (2016) 81500–81509. doi:10.1039/C6RA16279G.

[14] S. Wu, Y. Xiao, P. Song, C. Wang, Z. Yang, R.C.T. Slade, F. Zhao, Riboflavin-mediated extracellular electron transfer process involving Pachysolen tannophilus, Electrochim. Acta. 210 (2016) 117–121. doi:10.1016/j.electacta.2016.05.139.

[15] Y. Meng, X. Hun, Y. Zhang, X. Luo, Toehold-aided DNA recycling amplification using hemin and G-quadruplex reporter DNA on magnetic beads as tags for chemiluminescent determination of riboflavin, Microchim. Acta. 183 (2016) 2965–2971. doi:10.1007/s00604-016-1937-x.

[16] N. Song, C.J. Dares, M. V. Sheridan, T.J. Meyer, Proton-Coupled Electron Transfer Reduction of a Quinone by an Oxide-Bound Riboflavin Derivative, J. Phys. Chem. C. 120 (2016) 23984–23988.

doi:10.1021/acs.jpcc.6b08176.

[17] M. Roushani, A. Valipour, Voltammetric immunosensor for human chorionic gonadotropin using a glassy carbon electrode modified with silver nanoparticles and a nanocomposite composed of graphene, chitosan and ionic liquid, and using riboflavin as a redox probe, Microchim. Acta. 183 (2016) 845–853. doi:10.1007/s00604-015-1731-1.

[18] R. Celiešiūtė, A. Radzevič, A. Žukauskas, Š. Vaitekonis, R. Pauliukaite, A Strategy to Employ Polymerised Riboflavin in the Development of Electrochemical Biosensors, Electroanalysis. 29 (2017) 2071–2082. doi:10.1002/elan.201700218.

[19] A. Valipour, M. Roushani, Using silver nanoparticle and thiol graphene quantum dots nanocomposite as a substratum to load antibody for detection of hepatitis C virus core antigen: Electrochemical oxidation of riboflavin was used as redox probe, Biosens. Bioelectron. 89 (2017) 946–951. doi:10.1016/j.bios.2016.09.086.

[20] M. Roushani, Z. Abdi, Novel electrochemical sensor based on graphene quantum dots/riboflavin nanocomposite for the detection of persulfate, Sensors Actuators, B Chem. 201 (2014) 503–510. doi:10.1016/j.snb.2014.05.054.

[21] A. Radzevi??, G. Niaura, I. Ignatjev, T. Rakickas, R. Celie??i??t??, R. Pauliukaite, Electropolymerisation of the natural monomer riboflavin and its characterisation, Electrochim. Acta. 222 (2016) 1818–1830. doi:10.1016/j.electacta.2016.11.166.

[22] R.-W. Si, Y. Yang, Y.-Y. Yu, S. Han, C.-L. Zhang, D.-Z. Sun, D.-D. Zhai, X. Liu, Y.-C. Yong, Wiring Bacterial Electron Flow for Sensitive Whole-Cell Amperometric Detection of Riboflavin, Anal. Chem. 88 (2016) 11222–11228. doi:10.1021/acs.analchem.6b03538.

[23] S.L.J. Tan, R.D. Webster, Electrochemically induced chemically reversible proton-coupled electron transfer reactions of riboflavin (Vitamin B 2), J. Am. Chem. Soc. 134 (2012) 5954–5964. doi:10.1021/ja300191u.

[24] A. Kormányos, M.S. Hossain, G. Ghadimkhani, J.J. Johnson, C. Janáky, N.R. de Tacconi, F.W. Foss, Y. Paz, K. Rajeshwar, Flavin Derivatives with Tailored Redox Properties: Synthesis, Characterization, and Electrochemical Behavior, Chem. - A Eur. J. 22 (2016) 9209–9217. doi:10.1002/chem.201600207.

[25] P. Salvo, N. Calisi, B. Melai, B. Cortigiani, M. Mannini, A. Caneschi, G. Lorenzetti, C. Paoletti, T. Lomonaco, A. Paolicchi, I. Scataglini, V. Dini, M. Romanelli, R. Fuoco, F. Di Francesco, Temperature and pH sensors based on graphenic materials, Biosens. Bioelectron. 91 (2017) 870–877. doi:10.1016/j.bios.2017.01.062.

[26] G.K. Mani, K. Miyakoda, A. Saito, Y. Yasoda, K. Kajiwara, M. Kimura, K. Tsuchiya, Microneedle pH Sensor: Direct, Label-Free, Real-Time Detection of Cerebrospinal Fluid and Bladder pH, ACS Appl. Mater. Interfaces. 9 (2017) 21651–21659. doi:10.1021/acsami.7b04225.

[27] J. Yang, T.J. Kwak, X. Zhang, R. McClain, W.J. Chang, S. Gunasekaran, Digital pH Test Strips for In-Field pH Monitoring Using Iridium Oxide-Reduced Graphene Oxide Hybrid Thin Films, ACS Sensors. 1 (2016) 1235–1243. doi:10.1021/acssensors.6b00385.

[28] F.A. Fiorda, G.V. de Melo Pereira, V. Thomaz-Soccol, S.K. Rakshit, M.G.B. Pagnoncelli, L.P. de S. Vandenberghe, C.R. Soccol, Microbiological, biochemical, and functional aspects of sugary kefir fermentation - A review, Food Microbiol. 66 (2017) 86–95. doi:10.1016/j.fm.2017.04.004.

[29] O. Gul, M. Mortas, I. Atalar, M. Dervisoglu, T. Kahyaoglu, Manufacture and characterization of kefir made from cow and buffalo milk, using kefir grain and starter culture, J. Dairy Sci. 98 (2015) 1517–1525.

doi:10.3168/jds.2014-8755.

[30] D.D. Rosa, M.M.S. Dias, Ł.M. Grześkowiak, S.A. Reis, L.L. Conceição, M. do C.G. Peluzio, Milk kefir: nutritional, microbiological and health benefits, Nutr. Res. Rev. 30 (2017) 82–96. doi:10.1017/S0954422416000275.

[31] D. Laureys, L. De Vuyst, The water kefir grain inoculum determines the characteristics of the resulting water kefir fermentation process, J. Appl. Microbiol. 122 (2017) 719–732. doi:10.1111/jam.13370.

[32] B.C.T. Bourrie, B.P. Willing, P.D. Cotter, The microbiota and health promoting characteristics of the fermented beverage kefir, Front. Microbiol. 7 (2016) 1–17. doi:10.3389/fmicb.2016.00647.

[33] G. Satir, Z.B. Guzel-Seydim, How kefir fermentation can affect product composition?, Small Rumin. Res. 134 (2016) 1–7. doi:10.1016/j.smallrumres.2015.10.022.

[34] C.G. Tsiouris, M. Kelesi, G. Vasilopoulos, I. Kalemikerakis, E.G. Papageorgiou, The efficacy of probiotics as pharmacological treatment of cutaneous wounds: Meta-analysis of animal studies, Eur. J. Pharm. Sci. 104 (2017) 230–239. doi:10.1016/j.ejps.2017.04.002.

[35] D. Laureys, L. De Vuyst, Microbial species diversity, community dynamics, and metabolite kinetics of water Kefir fermentation, Appl. Environ. Microbiol. 80 (2014) 2564–2572. doi:10.1128/AEM.03978-13.

[36] A.L. Ntsame Affane, G.P. Fox, G.O. Sigge, M. Manley, T.J. Britz, Simultaneous prediction of acidity parameters (pH and titratable acidity) in Kefir using near infrared reflectance spectroscopy, Int. Dairy J. 21 (2011) 896–900. doi:10.1016/j.idairyj.2011.04.016.

[37] L. Qingwen, W. Yiming, L. Guoan, pH-Response of nanosized MnO2 prepared with solid state reaction route at room temperature, Sensors Actuators B Chem. 59 (1999) 42–47. doi:10.1016/S0925-4005(99)00189-6.

[38] J. Yang, T.J. Kwak, X. Zhang, R. McClain, W.J. Chang, S. Gunasekaran, Digital pH Test Strips for In-Field pH Monitoring Using Iridium Oxide-Reduced Graphene Oxide Hybrid Thin Films, ACS Sensors. 1 (2016) 1235–1243. doi:10.1021/acssensors.6b00385.

[39] W.D. Huang, H. Cao, S. Deb, M. Chiao, J.C. Chiao, A flexible pH sensor based on the iridium oxide sensing film, Sensors Actuators, A Phys. 169 (2011) 1–11. doi:10.1016/j.sna.2011.05.016.

[40] L. Santos, J.P. Neto, A. Crespo, D. Nunes, N. Costa, I.M. Fonseca, P. Barquinha, L. Pereira, J. Silva, R. Martins, E. Fortunato, WO3 nanoparticle-based conformable pH sensor, ACS Appl. Mater. Interfaces. 6 (2014) 12226–12234. doi:10.1021/am501724h.

[41] L. Maiolo, S. Mirabella, F. Maita, A. Alberti, A. Minotti, V. Strano, A. Pecora, Y. Shacham-Diamand, G. Fortunato, Flexible pH sensors based on polysilicon thin film transistors and ZnO nanowalls, Appl. Phys. Lett. 105 (2014). doi:10.1063/1.4894805.

[42] A. Anderson, J. Phair, J. Benson, B. Meenan, J. Davis, Investigating the use of endogenous quinoid moieties on carbon fibre as means of developing micro pH sensors, Mater. Sci. Eng. C. 43 (2014) 533–537. doi:10.1016/j.msec.2014.07.038.

[43] V.G.H. Lafitte, W. Wang, A.S. Yashina, N.S. Lawrence, Anthraquinone-ferrocene film electrodes: Utility in pH and oxygen sensing, Electrochem. Commun. 10 (2008) 1831–1834. doi:10.1016/j.elecom.2008.09.031.

[44] I. Streeter, H. Leventis, G. Wildgoose, M. Pandurangappa, N. Lawrence, L. Jiang, T.J. Jones, R. Compton, A sensitive reagentless pH probe with a ca. 120 mV/pH unit response, J. Solid State Electrochem. 8 (2004). http://link.springer.com/10.1007/s10008-004-0536-7 (accessed October 15, 2015).

[45] L. Xiong, C. Batchelor-Mcauley, R.G. Compton, Calibrationless pH sensors based on nitrosophenyl and

ferrocenyl co-modified screen printed electrodes, Sensors Actuators, B Chem. 159 (2011) 251–255. doi:10.1016/j.snb.2011.06.082.

[46] J.S.N. Dutt, M.F. Cardosi, S. Wilkins, C. Livingstone, J. Davis, Characterisation of carbon fibre composites for decentralised biomedical testing, Mater. Chem. Phys. 97 (2006) 267–272. doi:10.1016/j.matchemphys.2005.08.021.

[47] M. Bejugam, S. Sewitz, P.S. Shirude, R. Rodriguez, R. Shahid, S. Balasubramanian, Trisubstituted isoalloxazines as a new class of G-quadruplex binding ligands: Small molecule regulation of c-kit oncogene expression, J. Am. Chem. Soc. 129 (2007) 12926–12927. doi:10.1021/ja075881p.

[48] I.A. Cowden, W.B., Halladay, P.K, Cunningham, R.B, Hunt, N.H, Clark, Flavins as Potential Antimalarials. 2. 3-Methyl-lO-(substituted-phenyl)flavins, J. Med. Chem. 34 (1991) 1819.

[49] H. Faki, The development & evaluation of photoantimicrobial isoalloxazine dyes towards infection control, University of Central Lancashire, 2017.

[50] Y. Yang, Y. Wu, Y. Hu, Y. Cao, C.L. Poh, B. Cao, H. Song, Engineering Electrode-Attached Microbial Consortia for High-Performance Xylose-Fed Microbial Fuel Cell, ACS Catal. 5 (2015) 6937–6945. doi:10.1021/acscatal.5b01733.

[51] T.M. Pan, C.W. Wang, S. Mondal, S.T. Pang, Super-Nernstian sensitivity in microfabricated electrochemical pH sensor based on CeTixOyfilm for biofluid monitoring, Electrochim. Acta. 261 (2018) 482–490. doi:10.1016/j.electacta.2017.12.163.

[52] W. Lonsdale, M. Wajrak, K. Alameh, Manufacture and application of RuO2solid-state metal-oxide pH sensor to common beverages, Talanta. 180 (2018) 277–281. doi:10.1016/j.talanta.2017.12.070.

[53] Z. Zhu, X. Liu, Z. Ye, J. Zhang, F. Cao, J. Zhang, A fabrication of iridium oxide film pH micro-sensor on Pt ultramicroelectrode and its application on in-situ pH distribution of 316L stainless steel corrosion at open circuit potential, Sensors Actuators, B Chem. 255 (2018) 1974–1982. doi:10.1016/j.snb.2017.08.219.

[54] S. Chinnathambi, G.J.W. Euverink, Polyaniline functionalized electrochemically reduced graphene oxide chemiresistive sensor to monitor the pH in real time during microbial fermentations, Sensors Actuators, B Chem. 264 (2018) 38–44. doi:10.1016/j.snb.2018.02.087.

[55] L. Manjakkal, B. Sakthivel, N. Gopalakrishnan, R. Dahiya, Printed flexible electrochemical pH sensors based on CuO nanorods, Sensors Actuators, B Chem. 263 (2018) 50–58. doi:10.1016/j.snb.2018.02.092.

[56] W. Dang, L. Manjakkal, W.T. Navaraj, L. Lorenzelli, V. Vinciguerra, R. Dahiya, Stretchable wireless system for sweat pH monitoring, Biosens. Bioelectron. 107 (2018) 192–202. doi:10.1016/j.bios.2018.02.025.

[57] R. Cisternas, L. Ballesteros, M.L. Valenzuela, H. Kahlert, F. Scholz, Decreasing the time response of calibration-free pH sensors based on tungsten bronze nanocrystals, J. Electroanal. Chem. 801 (2017) 315–318. doi:10.1016/j.jelechem.2017.08.005.

[58] R. Sha, K. Komori, S. Badhulika, Amperometric pH Sensor Based on Graphene-Polyaniline Composite, IEEE Sens. J. 17 (2017) 5038–5043. doi:10.1109/JSEN.2017.2720634.

[59] J. Chou, S. Yan, Y. Liao, C. Lai, Characterization of Flexible Arrayed pH Sensor Based on Nickel Oxide Films, 18 (2018) 605–612.

[60] G.K. Mani, K. Miyakoda, A. Saito, Y. Yasoda, K. Kajiwara, M. Kimura, K. Tsuchiya, Microneedle pH Sensor: Direct, Label-Free, Real-Time Detection of Cerebrospinal Fluid and Bladder pH, ACS Appl. Mater. Interfaces. 9

(2017) 21651–21659. doi:10.1021/acsami.7b04225.

[61] N. Padmanathan, H. Shao, K.M. Razeeb, Multifunctional Nickel Phosphate Nano/Microflakes 3D Electrode for Electrochemical Energy Storage, Nonenzymatic Glucose, and Sweat pH Sensors, ACS Appl. Mater. Interfaces. 10 (2018) 8599–8610. doi:10.1021/acsami.7b17187.

[62] K. Chaisiwamongkhol, C. Batchelor-McAuley, R.G. Compton, Amperometric micro pH measurements in oxygenated saliva, Analyst. 142 (2017) 2828–2835. doi:10.1039/C7AN00809K.

[63] S. Bause, M. Decker, F. Gerlach, J. Näther, F. Köster, P. Neubauer, W. Vonau, Development of an iridium-based pH sensor for bioanalytical applications, J. Solid State Electrochem. (2017) 1–10. doi:10.1007/s10008-017-3721-1.

[64] N.M. Ahmed, E.A. Kabaa, M.S. Jaafar, A.F. Omar, Characteristics of Extended-Gate Field-Effect Transistor (EGFET) Based on Porous n-Type (111) Silicon for Use in pH Sensors, J. Electron. Mater. 46 (2017) 5804–5813. doi:10.1007/s11664-017-5604-8.

[65] G.K. Mani, M. Morohoshi, Y. Yasoda, S. Yokoyama, H. Kimura, K. Tsuchiya, ZnO-Based Microfluidic pH Sensor: A Versatile Approach for Quick Recognition of Circulating Tumor Cells in Blood, ACS Appl. Mater. Interfaces. 9 (2017) 5193–5203. doi:10.1021/acsami.6b16261.

[66] R. Rahimi, M. Ochoa, T. Parupudi, X. Zhao, I.K. Yazdi, M.R. Dokmeci, A. Tamayol, A. Khademhosseini, B. Ziaie, A low-cost flexible pH sensor array for wound assessment, Sensors Actuators, B Chem. 229 (2016) 609–617. doi:10.1016/j.snb.2015.12.082.

[67] M. Amiri, E. Amali, A. Nematollahzadeh, H. Salehniya, Poly-dopamine films: Voltammetric sensor for pH monitoring, Sensors Actuators, B Chem. 228 (2016) 53–58. doi:10.1016/j.snb.2016.01.012.